DYNAMICS OF ELECTRODIFFUSION FRICTION PROBES. I. SHAPE-DEPENDENT POTENTIOSTATIC TRANSIENT

Ondrej WEIN[1] and Vaclav SOBOLIK[2]

Institute of Chemical Process Fundamentals, Academy of Sciences of the Czech Republic, 165 02 Prague 6-Suchdol, Czech Republic; e-mail: [1]webox@icpf.cas.cz, [2] vs@icpf.cas.cz

Received October 18, 1996
Accepted December 19, 1996

An exact theory is given of the voltage-step transient under limiting diffusion conditions for an electrodiffusion friction probe of arbitrary convex shape. The actual transient courses are given for the strip, circular, elliptic, triangular, and rectangular probes of any orientation with respect to the flow direction. A simple formula for any probe with a single working electrode of convex shape is suggested to facilitate the calibration of electrodiffusion probes based on the voltage-step transient.
Key words: Unsteady diffusion layer; Limiting diffusion current; Wall shear rate.

The electrodiffusion (ED) technique, called sometimes the limiting diffusion current technique[1], is frequently used for various hydrodynamic studies, in particular for local measurements of wall friction parameters[2–6], represented either by the wall shear stress or wall shear rate. In typical hydrodynamic or calibration ED experiments, the active part of an electrodiffusion friction probe (EDFP) is the plane surface 1 (Fig. 1) of a thin metallic sheet, wire, or other profile, embedded in the insulating wall 2. From the electrochemical viewpoint, the EDFP is an electrolytic cell with a small working electrode 1 which controls the overall rate of electrolysis, and a larger grounded auxiliary electrode 3 made of a stainless steel capillary. The versatile EDFP as a whole is mounted flush with the wall 6 of a hydraulic set-up by means of a suitable fitting 5. The primary signal of an EDFP is the electric current $I = I(t)$.

For a given EDFP and a given electrolyte solution, this signal depends only on the velocity field in the diffusion layer of the working electrode, commonly represented by the surface field of the wall shear rate $\partial_z v_x|_{z=0} = q$. The calculation of $q = q(t)$ from the primary signal $I = I(t)$ can be based on either the complete theory of the process (including all the related parameters) or a suitable set of calibration data. In an oncoming series of papers, we suggest a combination of calibration experiments enabling the primary data of both the single and direction-sensitive (*i.e.* multi-segment) EDFP to be evaluated under unsteady-flow conditions, including transient (aperiodic) flows and fluctuating flows with large amplitudes.

The actual purpose of the present paper is to generalize the existing two-dimensional exact theory of the potentiostatic transient for EDFP with a single working electrode of convex shape.

THEORETICAL

Steady-State Calibration

Under steady-state flow conditions with constant q, the steady local limiting diffusion current density i is given by the well-known formula which follows[4,7] directly from the Faraday law of electrolysis for a couple of depolarizers, Ox + n e ↔ Red, and the classical Lévêque theory of convective diffusion:

$$i = i_{\mathrm{L}}(x) \equiv \alpha^{1/2} n\boldsymbol{F} c^{\mathrm{b}} D^{2/3} q^{1/3} x^{-1/3} , \quad \alpha^{1/2} = 9^{-1/3}/\Gamma\left(\tfrac{4}{3}\right) . \qquad (1)$$

Here, x stands for the distance between a point on the surface A of the working electrode and its forward edge taken in the flow direction (Fig. 2). Other quantities are specified in Symbols and Definitions.

The measurable steady total current I_{s} can be calculated by integrating Eq. (1) over A,

$$I_{\mathrm{s}} = \int\int_A i_{\mathrm{L}}(x)\, \mathrm{d}x\, \mathrm{d}y = k_{\mathrm{L}} q^{1/3} = \left(\tfrac{9}{4}\alpha\right)^{1/2} n\boldsymbol{F} c^{\mathrm{b}} D^{2/3} S_A L_{\mathrm{e}}^{-1/3} q^{1/3} , \qquad (2)$$

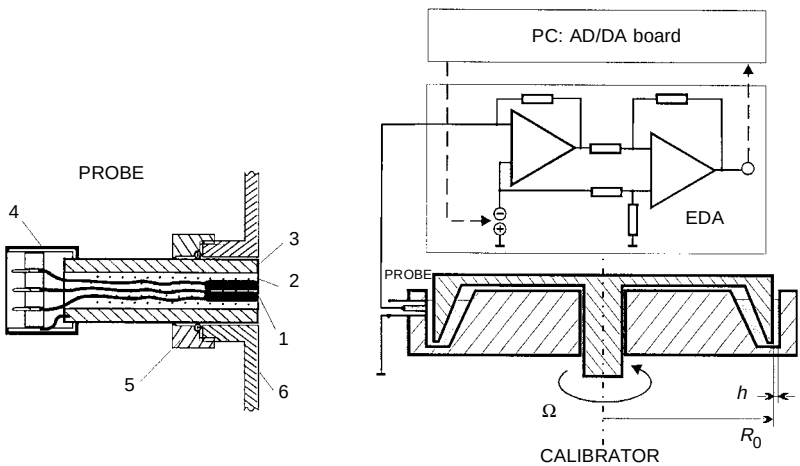

FIG. 1

Versatile multi-segment EDFP and the calibration set-up generating a steady viscometric flow in the gap between fixed (outer) and rotating (inner) cylinders. EDA: Electrodiffusion interface for bipolar potentiodynamic control and current/voltage converting, PROBE: 1 working electrodes, 2 insulating resin, 3 stainless steel capillary (holder and auxiliary electrode), 4 three-channel connector with a screening/grounding contact, 5 versatile fitting with O-ring, 6 wall of a hydraulic set-up (the CALIBRATOR in this case)

where the geometry and orientation of the electrode are represented by its area,

$$S_A = \int_0^W l(y)\,\mathrm{d}y \ , \tag{3a}$$

and equivalent transport length L_e,

$$L_e^{-1/3} = \int_0^W l^{2/3}\,\mathrm{d}y \Big/ \int_0^W l\,\mathrm{d}y \ . \tag{3b}$$

The function $l = l(y)$, $y \in (0,W)$ completely describes the relevant geometry of the oriented working electrode by giving the local transport lengths of infinitesimal strips parallel to the flow direction, as shown in Fig. 2. Note that, for any convex surface A, the function $l = l(y)$ displays only single local maximum L. This maximum transport length is related to the equivalent transport length by the geometrical simplex

$$\psi \equiv (L/L_e)^{2/3} = \left[\int_0^W (l/L)^{2/3}\,\mathrm{d}y \Big/ \int_0^W (l/L)\,\mathrm{d}y \right]^2 \ . \tag{3c}$$

Formula (*2*) in the form $I_s = k_L q^{1/3}$ with k_L taken from the theory, has frequently been used for determining shear rate $q(t) = (I(t)/k_L)^3$ from primary fluctuating data on the electric current $I = I(t)$. Such an approach, which assumes the electrodiffusion technique to be an absolute and quick (no delay) measuring method, is based on several assumptions:

1. No additional electrode reaction[8] (reduction of dissolved oxygen or traces of reducible organic compounds, electrolysis of water) occurs at the working electrode.

2. Various side effects, such as ohmic and charge-transfer resistances[7–10], surface blockage[11] or roughness[12], migration[7,13], longitudinal[14] and transversal[15] diffusion, anomalous velocity profile[16], are negligible.

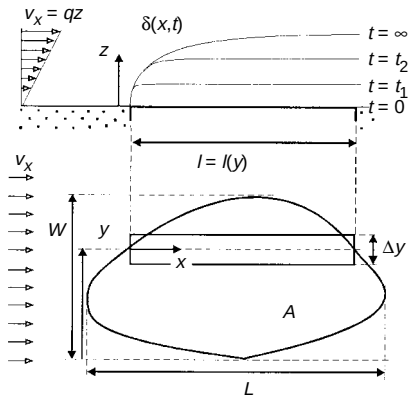

FIG. 2
Side and front view on a working electrode with surface A. $v_x(z)$ velocity profile within the diffusion layer of time-dependent thickness $\delta = \delta(x,t)$

3. All the calibration parameters $\{n\boldsymbol{F}, c^{\mathrm{b}}, S_A, D, l(y)\}$ are known with acceptable accuracy.

4. The changes of wall shear rate are so slow, or the sensor's response is so fast that the steady-state relation (*2*) can be used under unsteady-flow conditions within the frame of a so-called quasi-steady approximation.

Since some of the aforementioned assumption may not be fulfilled, the electrochemical system used for the ED measurements should be calibrated. There are three standard calibration experiments[4] supported by our ED software[17]:

1. Polarization (current–voltage) curve *I–U* in steady state at a given wall shear rate. The main purpose of this experiment is to check the limiting diffusion plateau and to adjust a suitable constant overpotential for hydrodynamic measurements[1].

2. Steady calibration curve I_s–q under steady limiting diffusion regime, *i.e.* at a suitable constant overpotential. The main purpose of this calibration is to check the bounds for the theoretical Lévêque proportionality $I_s \cong q^{1/3}$ and to determine the proportionality constant. Anyway, the side effects – free convection and lateral diffusion at low shear rates and ohmic or charge-transfer resistance at high shear rates – can be taken into account by an appropriate calibration formula[18] .

3. Voltage-step transient curve *I–t* under steady (non-zero) flow condition and a suitable constant overpotential *U*. This transient experiment can easily be run without a special potentiostat as it can be started by switching on the outer circuit to a predetermined constant overvoltage[4,19]. Under ideal limiting-diffusion conditions, *i.e.* with negligible ohmic and charge-transfer resistance, this process is known as the *potentiostatic transient*[7,20].

The first two mentioned calibration procedures aim at a correct interpretation of the ED experiments under steady-state conditions. The potentiostatic transient provides some information about dynamics of the EDFP.

Dynamic Calibration: Cottrell Asymptote and the Complete Transient

The response of the ED probe in the early stage of potentiostatic transient experiment, $t \to 0$ (under idealizing assumption of negligible ohmic and charge-transfer resistance, smooth surface, and high enough overvoltage), is given by the *Cottrell asymptote*[9,10,20]:

$$I(t) = k_{\mathrm{C}} t^{-1/2} \quad . \tag{4}$$

The transient experiment under ideal conditions provides the Cottrell coefficient $k_{\mathrm{C}} = \pi^{-1/2} n\boldsymbol{F} c^{\mathrm{b}} S_A D^{1/2}$. With lack of direct steady calibration data, it can serve for partial calibration[19], *e.g.* for a fairly accurate estimate of I_s at a given q. If both the steady and transient calibration data are available, they provide sufficient information about dynamics of ED probe under flow fluctuation[2–4,21,22].

The chance to determine the Cottrell coefficient by direct measurements under the Cottrellian regime is strongly limited by several factors:

1. The assumption $It^{1/2}$ = constant inevitably fails for $t \to 0$ because the initial current cannot be unlimited. When the diffusion resistance close to the working electrode is negligibly small, some other transport resistances in the electrolytic cell (ohmic, charge-transfer, *etc.*) will control the current at a given overvoltage.

2. There is an intrinsic uncertainty (of a few microseconds) about the "true starting instant" $t = 0$ of the transient process[7,8,20]; the impedance of the electrochemical system (including the capacitance of electric double layers), limited speed of spreading the concentration signal, and additional ohmic and charge-transfer resistances are neglected in the oversimplified Cottrell theory, Eq. (*4*).

3. There are some hardware limitations (delays of a few microseconds) of synchronizing the starting voltage step with the data acquisition system.

4. Additional ohmic and charge-transfer resistances, negligible at common steady or fluctuating flow measurements, can affect strongly (either suppress or enhance[9,10]) the transient signal within the range of higher current densities, *i.e.* for the early stage of transient experiments.

5. Surface roughness may strongly promote the currents by enhancing the effective area of the thin penetrating concentration boundary layer[12] which envelopes the actual microscopic surface. This effect can, however, be strongly suppressed by using the ED probes with properly polished bulk platinum[19] or lithography-devised microelectrodes[22].

6. At longer times, the transient currents deviate from the Cottrell asymptote because of convection effects. Ultimately, the steady convective diffusion governs the entire process and the currents reach their steady, Lévêque asymptote according to Eq. (*2*).

It would be preferable to record the overall transient process and to treat the full-range primary transient data within the frame of a complete theory for accurate determination of both the asymptotic parameters k_C, I_s. In particular, it is quite reasonable to use the well-known theory of transient convective diffusion[23–25] in analysing the transient data within the region of lower current densities where the extent of secondary effects is comparable to those at the constant-voltage ED hydrodynamic measurements.

A suitable combination of the mentioned two quantities is the transient time t_0, the time coordinate of the cross-section of the Cottrell (penetration) and Lévêque (steady) asymptotes, see also Fig. 3. From the definition $I_s = k_C t_0^{-1/2}$, we obtain:

$$t_0 = t_0(L_e) \equiv \beta\tau(L_e) = \left(\tfrac{9}{4}\pi\alpha\psi\right)^{-1}\tau(L) \quad . \qquad (5)$$

By using the concept of potentiostatic transient time t_0, the existing two-dimensional exact theory of the potentiostatic transient[25] can readily be extented for EDFP with a single convex working electrode of any shape as both the shape and orientation are completely characterized by the function $l = l(y)$.

Fundamental Transformation for Arbitrary Convex Surface

Let us assume that the surface distribution of the local current density during the potentiostatic transient process, $i = i(x,y,t)$, is known, and can be expressed in the form

$$i(x,y,t)/i_L(x) = N[\vartheta(x)] \ . \tag{6}$$

The variables N and $\vartheta = \vartheta(x) = \pi\alpha t/\tau(x)$ are normalized in such a way, that both the Cottrell and Lévêque asymptotes can be expressed in the following simple way:

$$N[\vartheta] \approx \begin{cases} \vartheta^{-1/2} \ , & \vartheta \to 0 \\ 1 \ , & \vartheta \to \infty \ . \end{cases} \tag{7}$$

By using the obvious proportionalities $i_L(x)/i_L(a) = (x/a)^{-1/3}$, $\vartheta(x)/\vartheta(a) = (x/a)^{-2/3}$ for any x, a, the transient current $I = I(t)$ can be calculated according to the scheme

$$\begin{aligned} I(t)/I_s &= \int\int_A N[\vartheta(x)] i_L(x)\, \mathrm{d}x\, \mathrm{d}y / \int\int_A i_L(x)\, \mathrm{d}x\, \mathrm{d}y = \\ &= \int_0^W N_m[\vartheta(L)(l/L)^{-2/3}] l^{2/3}\, \mathrm{d}y / \int_0^W l^{2/3}\, \mathrm{d}y \equiv M_A^*[\vartheta(L)] \ , \end{aligned} \tag{8}$$

where $\vartheta(L) = \pi\alpha t/\tau(L)$, and

$$N_m[\vartheta] = \int_0^l N[(x/l)^{-2/3}\vartheta] x^{-1/3}\, \mathrm{d}x / \int_0^l x^{-1/3}\, \mathrm{d}x = \int_0^1 N[\vartheta s^{-1}]\, \mathrm{d}s \ . \tag{9}$$

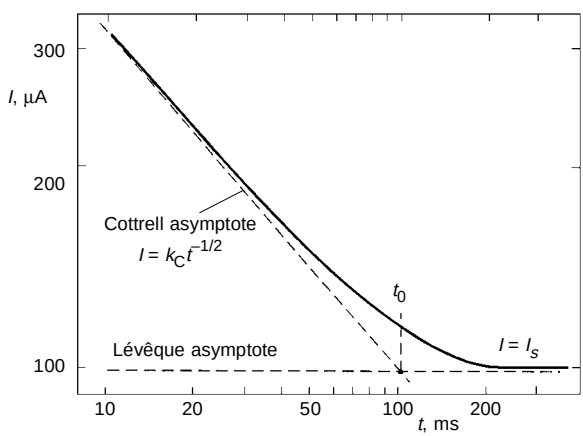

FIG. 3
Definition of the transient time t_0 for given asymptotic parameters k_C and I_s

The new choice of normalized time variable for the electrode as a whole, according to the definition (*5*) of the potentiostatic transient time $t_0 = t_0(L_e)$,

$$\theta = \theta(L_e) \equiv t/t_0(L_e) = \tfrac{9}{4}\vartheta(L_e) = \tfrac{9}{4}\psi\vartheta(L) \ , \qquad (10)$$

is reflected by the corresponding transformation $I(t)/I_s = M_A^*[(\frac{9}{4}\psi)^{-1}\theta(L_e)]$. For an infinite strip of the transport length L, we have $l(y)/L = 1$, $\psi = 1$ and, therefore,

$$I(t)/I_s = M[\theta] = N_m\,[\tfrac{4}{9}\,\theta] = \int_0^1 N\,[\tfrac{4}{9}\,\theta s^{-1}]\,\mathrm{d}s \ . \qquad (11)$$

By combining Eqs (*8*)–(*11*), the transient characteristic for any surface A can be written as:

$$I(t)/I_s \equiv M_A\,[\theta] = \int_0^W M\,[(l/L_e)^{-2/3}\theta]\,l^{2/3}\,\mathrm{d}y / \int_0^W l^{2/3}\,\mathrm{d}y \qquad (12)$$

which expresses the effect of the directionally dependent shape of working electrode on its normalized transient characteristic.

Some algebraic symmetries of the functional $M_A[\theta]$ with respect to its argument $l = l(y)$ are used in the following analysis. Neither ψ nor $M_A[\theta]$ change under the two-parametric affine transformation $l(y) \to al(by)$. The only change $\theta(x) \to \theta(ax) = a^{-2/3}\theta(x)$ reflects the size dependence of the transient time t_0.

Transient Characteristic for an Infinite Strip Surface

The transient mass transfer after a step change of the wall concentration from an initial value c^b to zero, within the approximation of concentration boundary layer (high enough qL^2/D), was originally studied[25] for an infinite strip of a constant transport length $l(y) = L$. The corresponding parabolic boundary-value problem,

$$\partial_t c + qz\partial_x c = D\partial_{zz} c \qquad (13a)$$

$$c = c^b \ ; \quad \text{for } (z \to \infty) \text{ or } (t < 0) \text{ or } (x \to 0) \text{ and } (z > 0) \qquad (13b)$$

$$c = 0 \ ; \quad \text{for } (x > 0) \text{ and } (z = 0) \ , \qquad (13c)$$

can be solved analytically[23,24] to provide the surface distribution of local current densities in the form of a slow convergent series:

$$N[\vartheta(x)] = 1 + 9^{2/3}\,\Gamma(\tfrac{4}{3}) \sum_{n=1}^{\infty} a_n^{-1} \exp\left(-\tfrac{2}{3}\vartheta_n^3\right) \mathrm{Ai}(\vartheta_n^2) \qquad (14a)$$

$$\vartheta_n = a_n 9^{-1/3} (\alpha\pi)^{-1}\, \vartheta(x) \ , \qquad (14b)$$

where $-a_n < 0$ stand for the zeroes of the Airy function, $\mathrm{Ai}(-a_n) = 0$. This series was integrated numerically according to the definitions (*9*), (*11*) and the result was expressed with an accuracy to 8 valid decimal digits by the empirical formulas:

$$M(\theta) = \begin{cases} \theta^{-1/2} + \frac{4}{27}(1 + k_0)\theta - \varepsilon_0(\theta) \ ; & \text{for } \theta < \frac{9}{4} \\ 1 + \varepsilon_\infty(\theta) \ ; & \text{for } \theta > \frac{9}{4} \end{cases} \qquad (15)$$

$$k_0 = 3\int_0^\infty (N[\vartheta] - \vartheta^{-1/2})\vartheta^{-2}\,\mathrm{d}\vartheta = 0.0199693\ldots \qquad (16a)$$

$$\varepsilon_0(\theta) = E_0 / \exp\left[(\theta^{-1} - \tfrac{4}{9}) / \sum_{k=0..4} \varepsilon_{0,k}\theta^{2k}\right] \qquad (16b)$$

$$\varepsilon_\infty(\theta) = \exp\left(-E_\infty\theta^3\right) \sum_{k=0..4} \varepsilon_{\infty,k}\theta^{-1-3k} \ , \qquad (16c)$$

with the parameters given in Table I. The exact course of $N = N[\vartheta]$ lies close (with deviations below 4%) to the simple prediction based on the concept of travelling diffusion wave[25,26],

$$N[\vartheta] \approx \begin{cases} \vartheta^{-1/2} \ ; & \text{for } \vartheta < 1 \\ 1 \ ; & \text{for } \vartheta > 1 \ , \end{cases} \qquad (17)$$

which provides an approximation to $M[\theta]$ by the simple form

$$M[\theta] = \begin{cases} \theta^{-1/2} + \frac{4}{27}\theta \ ; & \text{for } \theta < \frac{9}{4} \\ 1 \ ; & \text{for } \theta > \frac{9}{4} \end{cases} \qquad (18)$$

corresponding to Eqs (*15*) with $k_0 = 0$, $\varepsilon_0(\theta) = 0$, $\varepsilon_\infty(\theta) = 0$. The maximum difference between this "rough" approximation and the exact result for the strip is less than 0.3%.

With the known transient function $M[\theta]$ for infinite strips, $M_A[\theta]$ can be calculated for any convex surface A from Eq. (*12*).

Circles and Ellipses

Both the general functionals (*3c*), (*12*) are ratios of integrals of $l = l(y)$ over the domain $y \in (0,W)$. It is obvious from the circular symmetry, $l(2R - y) = l(y)$, and from the additivity of both the numerators and denominators in the functionals (*3c*), (*12*) that the integration over the subdomain, $y \in (0,W/2)$, where $W = L = 2R$, will provide the same result as for the entire domain, see also Fig. 4. The shape characteristic for the circular contour can be written as $l(y)/L = (1 - b(y - a)^2)^{1/2}$, where $b = R^{-2}$, $a = R$. The substitution $l(y)/L = s^{1/2}$, *i.e.* $dy/W \cong (1 - s)^{-1/2}\, ds$, transforms the original integrals in Eqs (*3c*) and (*12*) to quadratures:

TABLE I
Coefficients of the empirical approximations (*16b*), (*16c*) for the local transient function $N=N[\vartheta]$.

E_0	3.704842E–3	E_∞	0.2249143
$\varepsilon_{0,0}$	0.9912E–2	$\varepsilon_{\infty,0}$	0.01778242
$\varepsilon_{0,1}$	1.483887E–2	$\varepsilon_{\infty,1}$	1.313781
$\varepsilon_{0,2}$	–2.479827E–3	$\varepsilon_{\infty,2}$	–9.53622
$\varepsilon_{0,3}$	2.20265E–4	$\varepsilon_{\infty,3}$	49.87767
$\varepsilon_{0,4}$	–7.42231E–6	$\varepsilon_{\infty,4}$	–122.8633

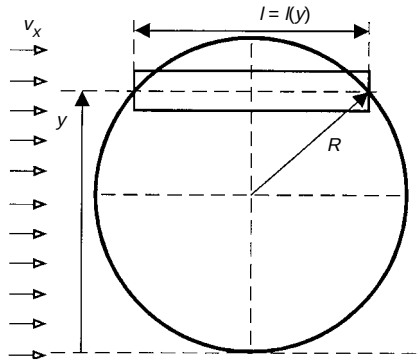

FIG. 4
The distribution function $l = l(y)$ for a circle

$$\psi_C = \left[\int_0^1 s^{1/3}(1-s)^{-1/2}\,\mathrm{d}s / \int_0^1 s^{1/2}\,(1-s)^{-1/2}\,\mathrm{d}s \right]^2 = 1.1474442\ldots \qquad (19a)$$

$$M_C[\theta] = \int_0^1 M\,[\psi_C^{-1}\theta s^{-1/3}]s^{1/3}\,(1-s)^{-1/2}\,\mathrm{d}s / \int_0^1 s^{1/3}\,(1-s)^{-1/2}\,\mathrm{d}s\ . \qquad (19b)$$

The accuracy of this quadrature with singularities on the boundaries was improved by using asymptotic formulas in the bounding regions, $\varepsilon \to 0$:

$$\int_0^{\varepsilon} M\,[as^{-1/3}]s^{1/3}\,(1-s)^{-1/2}\,\mathrm{d}s \approx a^{-1/2}\varepsilon^{3/2}\,(\tfrac{2}{3} + \tfrac{1}{5}\varepsilon) \qquad (20a)$$

$$\int_{1-\varepsilon}^1 M\,[as^{-1/3}]s^{1/3}\,(1-s)^{-1/2}\,\mathrm{d}s \approx M\,[a]\,2\varepsilon^{1/2}\ . \qquad (20b)$$

Selected numerical data on $M_C[\theta]$ are given in Table II.

For an ellipse of any orientation of its main halfaxis with respect to flow direction, the distribution of local transport lengths can be expressed in the same form as for the circle, $l(y)/L = (1 - b(y - a)^2)^{1/2}$, with the parameters L, b, a which depend both on the size and orientation of the ellipse. The transversal scaling factor has no effect on the ratio of the two integrals along the same domain and, hence, the resulting transient characteristic is the same as that for the circle. The transport length L_e for an ellipse contour of varying orientation is given by the formula

$$L_e = \psi_C^{-3/2} 2L_0\,(1 + \kappa^2)^{1/2}/(1 + \kappa^2 L_0^2/W_0^2)^{1/2}\ , \qquad (21)$$

where L_0, W_0 characterize the size and ϕ, $\kappa = \tan(\phi)$, the orientation of the given ellipse (Fig. 5).

Triangles

For a right-angled triangle of length L and width W, we have $l(y)/L = y/W = Y$ and hence, for $\theta = \theta(L_e) = \theta(\psi_T^{-3/2}L)$,

$$\psi_T = \left(\int_0^1 Y^{2/3}\,\mathrm{d}Y / \int_0^1 Y\,\mathrm{d}Y \right)^2 = \tfrac{36}{25} \qquad (22a)$$

TABLE II
Exact data on transient characteristics $M_A(\theta)$, obtained by numerical integration

$\theta^{3/2}$	$M_W(\theta)$	$M_S(\theta)$	$M_C(\theta)$	$M_T(\theta)$
	Eq. (*18*)	strips	circles	triangles
0.00	∞	∞	∞	∞
0.25	1.64619	1.64737	1.64956	1.65616
0.50	1.35325	1.35511	1.35849	1.36805
0.75	1.22294	1.22538	1.22967	1.24099
1.00	1.14815	1.15111	1.15609	1.16840
1.25	1.10023	1.10366	1.10912	1.12185
1.50	1.06771	1.07159	1.07731	1.09000
1.75	1.04497	1.04926	1.05502	1.06731
2.00	1.02887	1.03355	1.03911	1.05072
2.25	1.01752	1.02251	1.02766	1.03837
2.50	1.00970	1.01484	1.01941	1.02907
2.75	1.00456	1.00960	1.01349	1.02202
3.00	1.00152	1.00609	1.00928	1.01665
3.25	1.00016	1.00378	1.00631	1.01255
3.50	1.00015	1.00229	1.00424	1.00943
3.75	1.00000	1.00136	1.00282	1.00706
4.00	1.00000	1.00079	1.00185	1.00526
4.25	1.00000	1.00045	1.00120	1.00389
4.50	1.00000	1.00025	1.00077	1.00287
4.75	1.00000	1.00014	1.00050	1.00211
5.00	1.00000	1.00007	1.00032	1.00153
5.25	1.00000	1.00004	1.00020	1.00111
5.50	1.00000	1.00002	1.00013	1.00080
5.75	1.00000	1.00001	1.00009	1.00057
6.00	1.00000	1.00000	1.00006	1.00041

$$M_T[\theta] = \int_0^1 M[\psi_T^{-1}\theta Y^{-2/3}] Y^{2/3}\,\mathrm{d}Y / \int_0^1 Y^{2/3}\,\mathrm{d}Y = \int_0^1 M[\psi_T^{-1}\theta s^{-2/5}]\,\mathrm{d}s \ . \qquad (22b)$$

The characteristics L, ψ_T do not depend on the triangle width W. It is obvious from Fig. 6 that $l = l(y)$ for a general triangle A is the same as for the pair A' of two right-angled triangles with common value of L and of widths w_1, w_2. Hence, the transient characteristic $M_T[\theta]$ is the same for any triangle. Selected numerical data on $M_T[\theta]$ are given in Table II.

Rectangles

A probe of a rectangular shape A, characterized by its lengths $L_0 \geq w_0$ and the inclination angle ϕ, is shown in Fig. 7. By transforming A to the trapezoid A' with the same $l = l(y)$ characteristic and using the additivity of the individual surface integrals in (*2*) and (*12*), it is easy to obtain the following final expressions by applying the results for the strip and triangle:

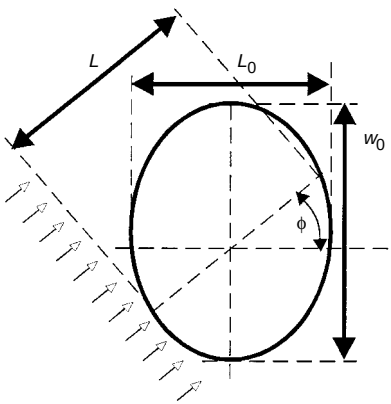

FIG. 5
Transport parameters for an ellipse aslant to the flow direction

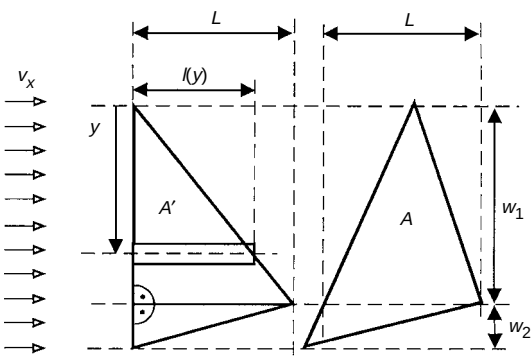

FIG. 6
The distribution function $l = l(y)$ for a triangle

$$\psi_R = \left[\left(w_S + \tfrac{6}{5} w_T\right)\left(w_S + w_T\right)\right]^2 \qquad (23a)$$

$$M_R[\theta] = \left(w_S M[\psi_R^{-1}\theta] + \tfrac{6}{5} w_T \int_0^1 M_T[\psi_R^{-1}\theta s^{-2/5}]\, \mathrm{d}s\right)\left(w_S + \tfrac{6}{5} w_T\right), \qquad (23b)$$

where $\theta = \theta(L_e)$, and

$$L = \min\left\{L_0/\cos(\phi)\,;\quad w_0/\sin(\phi)\right\} \qquad (24a)$$

$$w_T = \min\left\{L_0 \sin(\phi)\,;\quad w_0 \cos(\phi)\right\} \qquad (24b)$$

$$w_S = |L_0 \sin(\phi) - w_0 \cos(\phi)| \qquad (24c)$$

$$L_e = \psi_R^{-3/2} L\ . \qquad (24d)$$

The resulting transient characteristics for a revolving rectangle change within the limits $M_A(\theta) = M(\theta)$ for a two-dimensional strip

$$\left\{\phi = 0\,,\ L = L_0\,,\ w_T = 0\,,\ w_S = w_0\right\} \text{ or } \left\{\phi = \pi/2\,,\ L = w_0\,,\ w_T = 0\,,\ w_S = L_0\right\}\,,$$

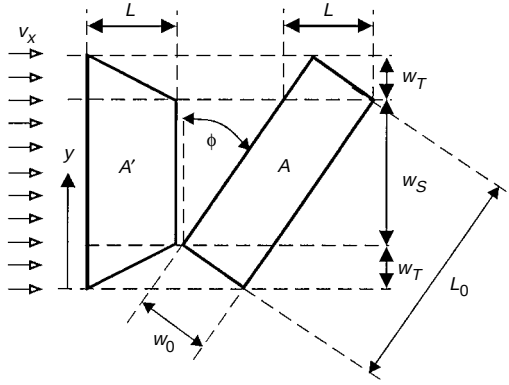

FIG. 7
Transport parameters for a rectangle aslant to the flow direction

and $M_A(\theta) = M_T(\theta)$ for a pair of identical triangles

$$\left\{\phi = \arctan\,(w_0/L_0)\,,\ w_S = 0\,,\ L = (L_0^2 + w_0^2)^{1/2}\,,\ w_T = (L_0^{-2} + w_0^{-2})^{-1/2}\right\}\ .$$

RESULTS AND DISCUSSION

Representation of Theoretical Results

A selected choice of exact data about the transient characteristics is given in Table II and Fig. 8. The data (generated by numerical integration for θ changing from 0 to 8 at steps of 0.025) were further treated to obtain simple empirical representations which can easily be implemented into computer programs[17] for automated control and treating of the electrodiffusion calibration experiments. The choice of the empirical formula with four adjustable parameters b_1, b_2, b_3, θ_0,

$$M_f[\theta] \approx \begin{cases} \theta^{-1/2}\,(1 + b_1\theta^{3/2} + b_2\theta^{6/2} + b_3\theta^{9/2})\,; & \text{for } \theta < \theta_0 \\ 1 \qquad\qquad\qquad\qquad\qquad\quad\ ; & \text{for } \theta > \theta_0 \end{cases} \tag{25}$$

is motivated by the analytical result (*18*) for the travelling-wave approximation[25,26] which was already used in ED experiments[27,28]. The parameters of this formula given in Table III were adjusted by minimizing the maximum of the relative deviation Δ (see also Fig. 9):

$$\Delta = \Delta(\theta) \equiv M_A[\theta]/M_f[\theta] - 1\,,\quad \Delta_{\max} = \max\left\{|\Delta(\theta)|\right\}\ . \tag{26}$$

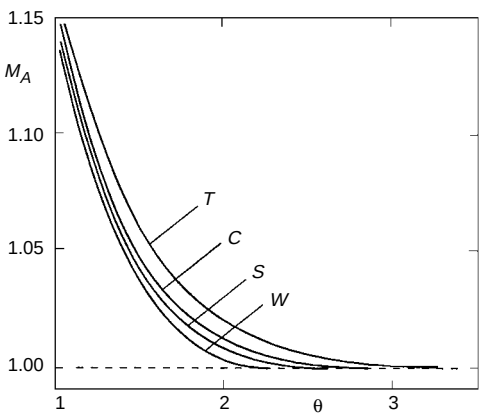

FIG. 8
Exact transient curves M_A for various *A*, see also Table II. *S* infinite strip (a rectangle with neglected transversal edge effects), *T* triangle of any orientation, *C* circle (and ellipse of any orientation), *W* travelling wave approximation, Eq. (*18*)

The common task of the data treatment is the extrapolation of the experimental transient data obtained for a finite time interval to the asymptotic regions $t \to 0$ (Cottrell asymptote, $I = k_C t^{-1/2}$), and $t \to \infty$ (Lévêque asymptote, $I = I_s$). It is obvious from the present theory that the transient current approaches rapidly the steady value I_s and hence it can be directly measured. On the other hand, the Cottrell coefficient can be obtained only by applying a suitable extrapolation procedure. The most suitable way of the data treatment aiming at the determination of k_C is to fit the data by a cubic polynomial in the coordinates $t^{1/2}I(t)$ *vs* $t^{3/2}$. This choice follows from the Eq. (*25*), which can also be written in the form

TABLE III
Polynomial approximations to $M_A(\theta)$ for strips, triangles and circles

Parameter	Strips new fit	Triangles new fit	Circles		
			new fit	old fit[27]	Eq. (*18*)
b_1	0.152770	0.173610	0.1518270	0.153465	0.148148
b_2	–0.000181	–0.005989	–0.000655	0	0
b_3	–0.000267	–0.000042	–0.000497	–0.000416	0
θ_0	2.48	3.22	2.73	2.58	2.25
X_0	3.90	5.80	4.5	4.15	3.28
$M_f[\theta_0]$	1.0020	0.9999	1.0016	1.0001	1.0000
Δ_{max}, %	0.11	0.07	0.09	0.42	0.98

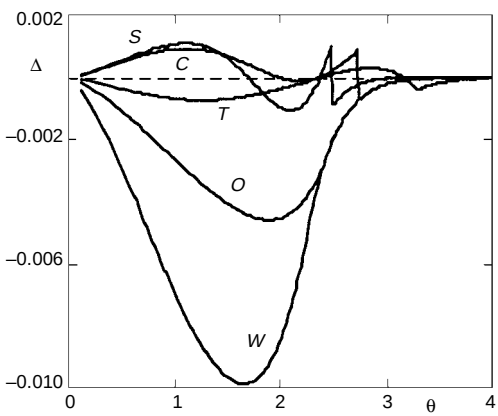

FIG. 9
Relative deviations of the polynomial approximations to $M_A(\theta)$, see also Table III. *O* the old fit for circle taken from[27], the other labels have the same meaning as in Fig. 8

$$Y = \begin{cases} 1 + b_1 X + b_2 X^2 + b_3 X^3 ; & \text{for } X < X_0 \\ X^{1/3} ; & \text{for } X > X_0 \end{cases} , \qquad (27)$$

where

$$Y = \theta^{1/2} M_A = t^{1/2}\, I(t)/k_C , \quad X = \theta^{3/2} = (t/t_0)^{3/2} = (I_s/k_C)^3 t^{3/2} , \qquad (28a,b)$$

and the coordinates $[Y_0 , X_0]$ of the cutting point (the beginning of the ultimate steady line $I = I_s$ within the accuracy of the approximation used) were given in Table III for various values of A, (Fig. 10). For a working electrode of a given shape, *i.e.* with known parameters b_k , X_0 in Eq. (*27*), the transient data treatment reduces to a non-linear least-squares fitting with only two free parameters, k_C, I_s, or $t_0 = (k_C/I_s)^2$.

An Example of Transient Data Treatment with Extrapolations

A set of transient data for several shear rates q obtained in a calibration set-up[19] is shown in Fig. 11. The EDFP used is equipped with a single circular electrode of diameter 0.5 mm. The EDFP operated under cathodic regime (U = –0.8 V) in an equimolar $K_4Fe(CN)_6/K_3Fe(CN)_6$ aqueous solution, c^b = 25 mol m^{-3}, containing 2% K_2SO_4 as a supporting electrolyte. The transient currents were measured with a 6-channel EDA electrodiffusion interface (Fig. 1), which operated in the range up to 1 000 μA.

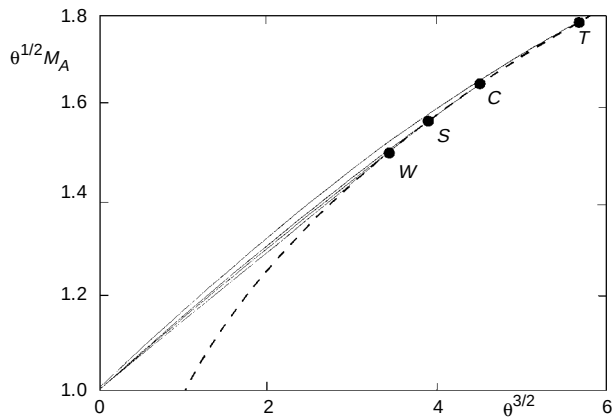

FIG. 10
Polynomial representations (*25*) of the transient curves, see also Table III. Labels have the same meaning as in Fig. 8, the dashed curve corresponds to the steady-state asymptote, M_A = 1

The normalized voltage output signal of ±5 V was sampled at a frequency of 2 kHz and digitized by using a 12-bit AD transducer.

The resulting transient data, serving originally[19] to confirm a good electrode quality in the region of higher current densities, are shown in Figs 11 and 12. A few first data in all the runs, for $t < 10$ ms, are distinguished in both the graphs by empty circles. It is obvious from Fig. 12 that these data display a systematic deviation from the Cottrell asymptote and should not be used for determining k_C. With the 1 000 μA current range and the 12-bit AD transducer, the digitized current signal was recorded with an error of $1000/2^{12} = 0.2$ μA, low enough to obtain fairly accurate transient currents at $I > 50$ μA, but inappropriate for measurements of steady currents in the region of 10–20 μA because of the data dispersion, obvious in Fig. 12. In spite of this noise, the statistical smoothing of the data by using Eq. (*27*) for the circle contour of the ED sensor provides very accurate estimates of the Cottrell coefficient k_C, given in Table IV.

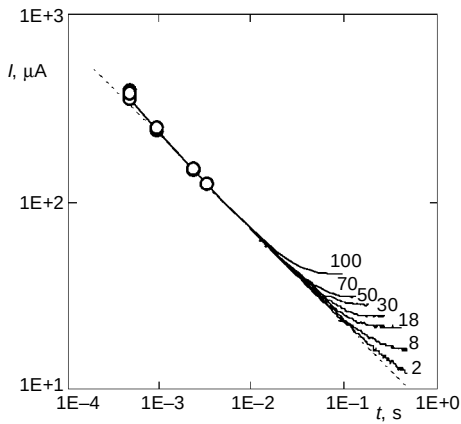

FIG. 11
Set of the potentiostatic transient curves for a circular ED probe[19] in primary coordinates. The data for $t < 10$ ms are distinguished by empty circles, labels give the shear rates (in s^{-1}) in the experimental runs, see also Table IV

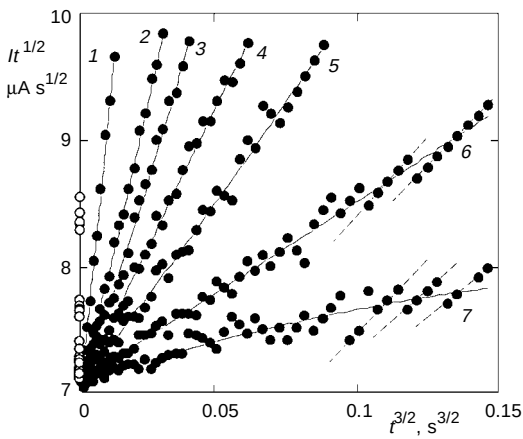

FIG. 12
Set of the potentiostatic transient curves for a circular ED probe[19] in modified coordinates. The data for $t < 10$ ms are distinguished by empty circles, labels identify the experimental runs in Table IV, dashed lines show selected curves I = const in the region of low currents

The accurate knowledge of the complete theory can serve for extrapolation of the early transient data, $t << t_0$, towards the steady asymptote. According to the theory, reflected by the approximate relation (*27*), the linear term of the expansion

$$It^{1/2} = k_C + B_1 t^{3/2} + B_2 t^{6/2} + B_3 t^{9/2} \quad , \tag{29}$$

where $B_i = b_i/t_0^{3i/2}$, can be used to predict I_s,

$$I_s^3 = \frac{k_C^2}{b_1} \left. \frac{\mathrm{d}It^{1/2}}{\mathrm{d}t^{3/2}} \right|_{t \to 0} = \frac{k_C^2}{b_1} B_1 \quad , \tag{30}$$

where B_1 is obtained by data fitting, and the shape-dependent coefficient b_1 is given in Table III. The extrapolation estimates of I_s (Table IV) agree very well with the experimentally determined values.

Equivalent Transport Length L_e and Form Parameter ψ

The equivalent transport length L_e was chosen in such a way that working electrodes of the same area under the same transport conditions (solution, flow speed) manifest the same steady current I_s and, hence, the same potentiostatic transient time t_0. The auxiliary form parameter $\psi = (L/L_e)^{2/3} \geq 1$ facilitates calculation of L_e from primary information, $l = l(y)$, about geometry of the oriented electrode (Fig. 2).

In particular, we have $L_e = 1.627R$ for a circular electrode of radius R, in agreement with the estimate by Hanratty and Riess, noted *e.g.* in[2,22]. The same estimate works

TABLE IV
Estimate of I_s from an early period of the transient data, $t << t_0$. $I_{s,fit}$ extrapolation according to Eq. (*30*); $I_{s,act}$ direct experimental values

Run No.	q, s^{-1}	k_C, μA $s^{1/2}$	B_1, μA s^{-1}	t_0, s	$I_{s,fit}$, μA	$I_{s,act}$, μA
1	470	7.015	208.1	0.0297	40.7	40.7
2	371	7.017	87.6	0.0529	30.5	30.8
3	291	7.018	63.0	0.0659	27.3	28.1
4	203	7.016	47.4	0.0796	24.9	24.7
5	127	7.045	29.3	0.110	21.2	21.5
6	63	7.071	14.8	0.174	16.9	16.6
7	14.3	7.071	7.36	0.277	13.4	

well even for the flows with apparent wall slip effects[27], *i.e.* for non-linear velocity profiles within the diffusion layer. The variations of L_e/L_0 with the flow direction ϕ are shown for a rectangular probe in Fig. 13.

The normalized courses of transient characteristics in Figs 8 and 10 show just the shape-dependent differences between two electrodes of the same transport length, L_e (or transient time, t_0). In most cases (except for the triangular electrode), these differences are negligible.

Note that when the potentiostatic transient time t_0 and steady-state current I_s are taken as the primary quantities from dynamic calibration experiments, the question of a characteristic electrode length become irrelevant.

Accuracy of Various Representations of the Transient Characteristics

The exact theory of the potentiostatic transient (neither in terms of local current densities[23,24] nor for the infinite strip sensor[25]) was used in rational treatment of the experimental data. The approximate formulas for the circular sensors[27], used in the ED software[17], deviate from the exact theory more than by 0.5% (see Table III and Fig. 9, old fit for the circle) and, hence, they are not suitable for accurate extrapolation procedures. On the other hand, the simplest approximation formula, based on the concept of travelling diffusion wave[25,26], does not deviate from the exact results for any convex electrode by more than 1.5%. The newly adjusted approximate formulas (Eqs (*27*), (*29*) and Table III), make it possible to determine the asymptotic parameters k_C, t_0, I_s by

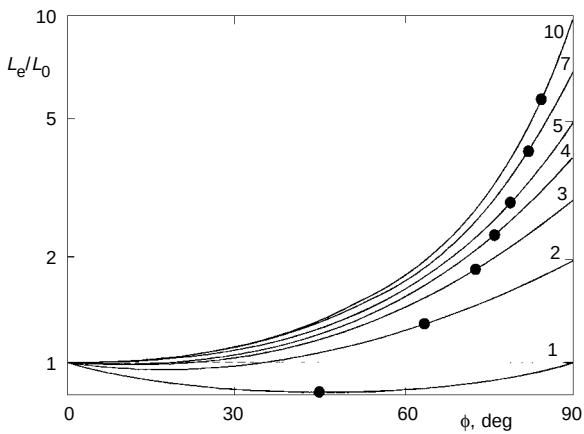

FIG. 13

Dependence of the effective transport length on the angle ϕ for rectangles aslant to the flow direction, see Fig. 7. The numerical labels of individual curves give the values of w_0/L_0, solid points indicate the critical angle, ϕ = arctan (w_0/L_0)

extrapolating the experimental data from the finite interval of times, $t \in (t_0,2t_0)$, and currents, $I < 1.5I_s$. The validity regions of the asymptotes are indicated in Figs 8 and 10 by dashed lines.

Experimental Conditions for an Accurate Dynamic Calibration

Both the range and sampling frequency of the measuring line (current follower – voltage amplifier – AD transducer – computer) for accurate transient measurements should be adjusted to cover the above-mentioned criteria. Unnecessarily high sampling frequencies or current ranges cannot provide accurate estimates of k_C, t_0, I_s because of low resolution of the digitized signal. The optimum range of the current follower should not exceed the level $2I_s$. At the same time, the current follower circuit itself must not restrict the currents range in the early stage of the transient experiment.

CONCLUSIONS

An exact theory of the potentiostatic transient (*i.e.* the voltage-step transient under the limiting-diffusion conditions) was presented for electrodiffusion friction probes with working electrode of any convex shape. In suitably normalized variables, M and θ, the shape dependence is very small and is displayed by the difference between the results for strip and triangular electrodes.

From the theoretical viewpoint, geometry of the electrode in flow of a given direction is specified by its area and the equivalent transport length L_e. For practical purposes – in flow measurements with a dynamically calibrated EDFP – the only meaningful calibration parameters are the steady limiting diffusion current I_s and the Cottrell coefficient k_C or the corresponding potentiostatic transient time $t_0 = (k_C/I_s)^2$. Note that this approach was originally suggested and applied by Pokryvaylo in his Ph.D. Thesis in 1967 (see ref.[4]).

For calibration experiments, the transient characteristics for strip, circle, ellipses, triangles and rectangles with arbitrary orientation to the flow direction were represented by simple but accurate polynomial formulas.

Statistical treatment of the voltage-step transient data with large dispersion, typical of computer-controlled experiments with a low-resolution AD board, can remarkably improve the accuracy of resulting calibration parameters k_C, I_s, and t_0, when based on the presented correct theory of the (complete) transient process.

SYMBOLS AND DEFINITIONS

A	surface of working electrode
b_i , B_i	coefficients of semiempirical represetantions, Eqs (*29*), (*30*), Table III
c^b	bulk concentration of depolarizer, mol m^{-3}
D	diffusivity of depolarizer, m^2 s^{-1}

$\boldsymbol{F}$	= 96484.56 C mol^{-1}, Faraday constant
h	width of gap between cylinders, m
i	local current density, A m^{-2}
i_L	local current density according to Lévêque theory, Eq. (*1*), A m^{-2}
$I = I(t)$	transient current under potentiostatic conditions, A
I_s	steady current according to Lévêque theory, Eq. (*2*), A
k_C	$= \pi^{-1/2} n\boldsymbol{F}c^b S_A D^{1/2}$, Cottrell coefficient in Eq. (*4*), A s$^{1/2}$
k_L	$= (\frac{9}{4}\alpha)^{1/2}\, n\boldsymbol{F}c^b\, D^{2/3}\, S_A\, L_e^{-1/3}$, Lévêque coefficient in Eq. (*2*), A s$^{1/3}$
$l = l(y)$	distribution of the local transport lengths, Fig. 2, m
L	maximum transport length, Fig. 2, m
L_0	width of a rectangle, Fig. 7, m
L_e	equivalent transport length, Eq. (*3b*), m
$M[\theta]$	$\equiv M_S[\theta]$, transient characteristic for a strip electrode, Eq. (*11*)
$M_A[\theta]$	shape-dependent transient characteristic for surface *A*, Eq. (*12*)
$M_f[\theta]$	approximate representation to transient characteristic, Eq. (*25*) and Table III
N	normalized local current density, Eq. (*6*)
$N[\vartheta(x)]$	local transient characteristic, Eq. (*6*)
$N_m[\vartheta(L)]$	transient characteristic for strip, Eq. (*9*)
n	number of electrons involved in electrode reaction
q	$= \Omega R_0/h$, wall shear rate in calibrator, s^{-1}
R	radius of circular ED probe, m
R_0	radius of rotating cylinder, m
S_A	area of A, m^2
t	time, s
t_0	$= (k_C/I_s)^2$, potentiostatic transient time, Eq. (*5*), s
U	overvoltage between working and auxiliary electrode, V
$v_x(z)$	velocity profile within diffusion layer of working electrode, m s^{-1}
w_0	length of rectangle, Fig. 7, m
w_S, w_T	partial widths of striplike and triangular parts of rectangle, Fig. 7, m
w_1, w_2	partial widths of triangle, Fig. 6, m
W	transport width of probe, Fig. 2, m
x	distance to forward edge, Fig. 2, m
X	modified coordinate for plotting transient currents, Eq. (*28b*)
y	transversal coordinate, Fig. 2, m
Y	modified coordinate for plotting transient currents, Eq. (*28a*)
z	distance to surface, Fig. 2, m
α	$= 9^{-2/3}/\Gamma^2(\frac{4}{3})$, constant of Lévêque theory, Eqs (*1*) and (*2*)
β	$= (\frac{9}{4}\pi\alpha)^{-1} = 0.48810398...$, constant in definition of transient time, Eq. (*5*)
$\Delta(\theta)$	relative error of approximation to transient characteristic, Eq. (*26*)
Δ_{max}	maximum to Δ
ε_0 , ε_∞	deviations from travelling wave approximation, Eq. (*18*)
θ	$= \theta(L_e)$, normalized time for whole electrode, Eq. (*10*)
ϑ	$= \vartheta(x) = \pi\alpha t/\tau(x)$, locally normalized time
κ	$= \tan(\phi)$, directional parameter for elliptical ED probe
$\tau(x)$	$= \sigma^2(x)/D = x^{2/3} q^{-2/3} D^{-1/3}$, modified local transient time, s
ϕ	angle of inclination, Figs 5 and 7
ψ	form parameter of oriented electrode, Eq. (*3c*)
Ω	angular speed of rotating cylinder, rad s^{-1}

Subscripts

A	any convex surface shape of ED probe
C	circles and ellipses of any orientation
R	rectangles of any orientation
S	infinite strip of any orientation
T	triangles of any orientation
W	travelling wave approximation

This work was partially supported by the Grant Agency of the Czech Republic under contract No. 104/95/0654 and by the Grant Agency of the Academy of Sciences of the Czech Republic under contract A4072502.

REFERENCES

1. Selman J. R., Tobias Ch. W.: Adv. Chem. Eng. *10*, 212 (1978).
2. Hanratty T. J., Campbell J. A. in: *Fluid Mechanics Measurements* (R. J. Goldstein, Ed.). Hemisphere Publ. Corp., Washington 1983.
3. Nakoryakov V. E., Burdukov A. P., Kashinsky O. N., Geshev P. I.: *Elektrodiffuzionnyi metod issledovaniya lokalnoi struktury turbulentnykh techenii*. Institute of Thermophysics, Novosibirsk 1986.
4. Pokryvaylo N. A., Wein O., Kovalevskaya N. D.: *Elektrodiffuzionnaya diagnostika techenii v suspenziyakh i polimernykh rastvorakh.* Nauka i Tekhnika, Minsk 1988.
5. *Proceedings of the 3rd International Workshop on Electrodiffusion Diagnostics of Flow* (C. Deslouis and B. Tribollet, Eds). Dourdan, France 1993.
6. *Proceedings of the 4th International Workshop on Electrochemical Flow Measurements* (K. Juttner, E. Heitz and B. Tribollet, Eds). Lahnstein, Germany 1996.
7. Newman J.: *Electrochemical Systems.* Prentice Hall, New Jersey 1973.
8. Vetter K. J.: *Electrochemical Kinetics.* Academic Press, New York 1967.
9. Wein O.: J. Appl. Electrochem. *21*, 1091 (1991).
10. Wein O.: Elektrokhimiya *29*, 8 (1993).
11. Wein O.: Collect. Czech. Chem. Commun. *58*, 496 (1993).
12. Wein O., Assaf F. H.: Collect. Czech. Chem. Commun. *52*, 848 (1987).
13. Wein O.: Collect. Czech. Chem. Commun. *53*, 697 (1988).
14. Newman J. S.: Adv. Electroanal. Chem. *6*, 279 (1973).
15. Wein O.: Collect. Czech. Chem. Commun. *53*, 1678 (1988).
16. Wein O., Kovalevskaya N. D.: Collect. Czech. Chem. Commun. *49*, 1289 (1984).
17. Wein O., Sobolik V.: *EDWORK91 Manual*. Tech. Report, Institute of Chemical Process Fundamentals, Prague 1992.
18. Wein O., Lindberg L. S., Sobolik V.: Presented at the *4th International Workshop on Electrochemical Flow Measurements. Lahnstein, Germany 1996.*
19. Sobolik V., Tihon J., Wein O., Wichterle K.: J. Appl. Electrochem., in press.
20. McDonald D. D.: *Transient Techniques in Electrochemistry*. Plenum Press, New York 1977.
21. Sobolik V., Wein O., Cermak J.: Collect. Czech. Chem. Commun. *52*, 913 (1987).
22. Deslouis C., Gill O., Tribollet B.: J. Fluid. Mech. *215*, 85 (1990).
23. Hudson J. L., Bankoff S. G.: Chem. Eng. Sci. *19*, 591 (1964).
24. Soliman M., Chambre P. L.: Int. J. Heat Mass Transfer *10*, 169 (1967).
25. Wein O.: Collect. Czech. Chem. Commun. *46*, 3209 (1981).

26. Wein O.: Collect. Czech. Chem. Commun. *61*, 1267 (1996).
27. Wein O., Kovalevskaya N. D.: Collect. Czech. Chem. Commun. *49*, 1297 (1984).
28. Wein O., Mitschka P., Tovchigrechko V. V., Kovalevskaya N. D., Yushkina T. V., Pokryvaylo N. A.: Chem. Eng. Commun. *32*, 153 (1985).